MultiCraft

International Journal of Engineering, Science and Technology
Vol. 4, No. 2, 2012, pp. 1-16

INTERNATIONAL JOURNAL OF ENGINEERING, SCIENCE AND TECHNOLOGY

www.ijest-ng.com

Prandtl number variation on transient forced convection flow in a fluid valve using nanofluid

Rehena Nasrin[1, *], M. A. Alim[1] and Ali J. Chamkha[2]

[1*]*Department of Mathematics, Bangladesh University of Engineering and Technology, Dhaka - 1000, BANGLADESH*
[2]*Manufacturing Engineering Department, The Public Authority for Applied Education and Training, Shuweikh 70654, KUWAIT*
[*] *Corresponding author: E-mail: rehena@math.buet.ac.bd*

Abstract

A transient numerical study is conducted to investigate the transport mechanism of forced convection in a fluid valve filled with water-CuO nanofluid. The flow enters from one inlet at the left with uniform temperature and velocity T_i and U_i, respectively, but can leave the valve through two outlets at the right. The upper and lower boundaries of the valve are heated with constant temperature T_h while the remaining walls are perfectly insulated. The numerical approach is based on the finite element technique with Galerkin's weighted residual simulation. Solutions are obtained for the variation of Prandtl number (Pr) while Reynolds number (Re) and solid volume fraction (ϕ) are fixed at 100 and 5%. The streamlines, isotherm plots, the local and average Nusselt number, mean temperature of the fluids (base fluid and nanofluid) and subdomain velocity with the variation of non-dimensional time (τ) are presented and discussed. It is found that the rate of heat transfer in the fluid valve reduces for longer time periods.

Keywords: Water-CuO nanofluid, forced convection, fluid valve, transient analysis.

1. Introduction

Recently, nanofluid technology has emerged as a new enhanced heat transfer technique. Nanofluid is made by adding nanoparticles and a surfactant into a base fluid can greatly enhance thermal conductivity and convective heat transfer. The diameters of nanoparticles are usually less than 100 nm which improves their suspension properties.

Investigations on natural convection of water-based nanofluids are conducted by Das and Ohal (2009) and Ogut (2009). Kumar et al. (2009) found the significant heat transfer enhancement by the dispersion of nanoparticles in the base fluid. Contradictory results were reported by Putra et al. (2003) based on experiment investigation in a cylindrical enclosure filled with water-Cu or water-Al_2O_3 nanofluids. They reported a systematic and definite deterioration in the heat transfer for the high Rayleigh numbers and the degree of deterioration depended on the density and concentration of the nanoparticles. Santra et al. (2008a, b) modeled the nanofluids as a non-Newtonian fluid and observed a systematic decrease of the heat transfer as the volume fraction of the nanofluids increased. The possible determining factors for the heat transfer reduction in nanofluids include the variations of the size, shape, and distribution of nanoparticles and uncertainties in the thermophysical properties of nanofluids. Most of the published papers are concerned with the analysis of natural convection heat transfer of nanofluids in square or rectangular enclosures; for example, Abu-Nada and Oztop (2009), Wong et al. (2008), Ghasemi and Aminossadati (2009), Muthtamilselvan et al. (2009) and Abu-Nada et al. (2010).

Many studies have described the larruping behaviors of nanofluids, such as their effective thermal conductivity under static conditions the convective heat transfer associated with fluid flow phenomena Dai et al. (2002, 2003). Liu & Liao (2008) studied the sorption and agglutination phenomenon of nanofluids on a plain heating surface during pool boiling. Dai et al. (2003) and Chen et al. (2004) investigated convective flow drag and heat transfer of CuO nanofluid in a small tube. Their results showed that the pressure drop of the nanofluid per unit length was greater than that of water. The pressure drop increased with the increasing weight concentration of nanoparticles. In the laminar flow region, the pressure drop had a linear relationship with the Re number,

while in the turbulent flow region, the pressure drop increased sharply with the increase of the *Re* number. The critical *Re* number became lower while the tube diameter was smaller. The convective heat transfer was obviously enhanced by adding nanoparticles. The nanoparticle weight concentration and flow status were the main factors influencing the heat transfer coefficient: the heat transfer coefficient increased with the increasing weight concentration, and the enhancement of heat transfer in the turbulent flow region wass greater than that in the laminar flow region. Pfautsch (2008) studied the characteristics, flow development, and heat transfer coefficient of nanofluids under laminar forced convection over a flat plate. He concluded that a significant increase in the heat transfer coefficient, about a 16% increase in the heat transfer coefficient for the water based nanofluid and about a 100% increase for the ethylene glycol based nanofluid. Wen and Ding (2004) reported an experiment on the convective heat transfer of water–γ-Al_2O_3 nanofluid.

Very recently, natural convection heat transfer in a nanofluid-filled trapezoidal enclosure was analyzed by Saleh et al. (2011). They found that acute sloping wall and Cu nanoparticles with high concentration were effective to enhance the rate of heat transfer. Moreover, Lin and Violi (2010) studied the problem of natural convection heat transfer of nanofluids in a vertical cavity where the effects of non-uniform particle diameter and temperature on thermal conductivity were shown.

Up to now, all the nanofluids in the existing researches used a surfactant to help nanoparticle suspending. Due to the stickiness of the surfactant, the sedimentation on the tube wall became colloid and was difficult to clear. The nanoparticles in the sedimentation could not suspend again. This kind of nanofluid would jam pipes during a prolonged period of operation. In order to overcome this disadvantage, our study used CuO nanoparticle suspensions (consisting of de-ionized water and nanoparticles without surfactant). During the flow process, the good suspension properties remained. So far, there is no research on the analysis of transient forced convective heat transfer on nanofluid in a fluid valve. Therefore, transient forced convection also becomes a crucial point of this study. The main issues discussed in this paper are: comparisons of the convective flow drag and heat transfer characteristics between pure water and water-CuO nanofluid in the fluid valve.

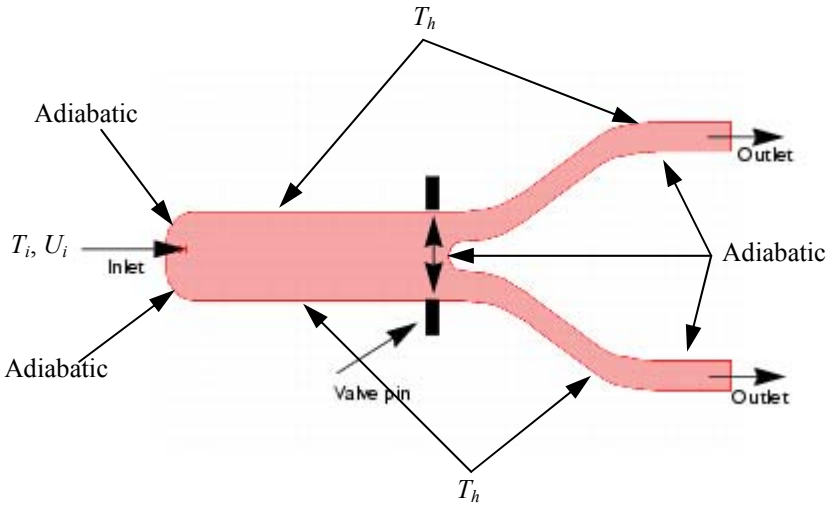

Fig. 1: Depiction of the geometry and the operation of the fluid valve

2. Physical Configuration

Fig. 1 shows a schematic diagram of the fluid valve. The model describes a valve where it is possible to direct the flow into one of two channels. Flow of varying degrees can also occur in both channels during the opening and closing stages. Flow enters from one inlet at the left, but can leave the valve through two outlets at the right. The choice of outlet depends upon the position of the valve pin. In this model, two valve pins oscillate from in front of one outlet channel to being in front of the other. Sometimes flow is possible through both outlets, depending on the position of the pins. The valve pin moves according to a sinusoidal function of time. The inlet fluid velocity and temperature are U_i and T_i respectively. The upper and lower boundaries of the valve are heated with constant temperature T_h while the remaining walls are perfectly insulated. The fluid in the valve is water-based nanofluid containing CuO nanoparticles.

3. Mathematical Formulation

In the present problem, it is considered that the flow is steady, two-dimensional, laminar, incompressible and there is no viscous dissipation**.** The radiation effect is neglected. The governing equations under Boussinesq approximation are as follows

$$\frac{\partial u}{\partial x}+\frac{\partial v}{\partial y}=0 \tag{1}$$

$$\rho_{nf}\left(\frac{\partial u}{\partial t}+u\frac{\partial u}{\partial x}+v\frac{\partial u}{\partial y}\right)=-\frac{\partial p}{\partial x}+\mu_{nf}\left(\frac{\partial^2 u}{\partial x^2}+\frac{\partial^2 u}{\partial y^2}\right) \tag{2}$$

$$\rho_{nf}\left(\frac{\partial v}{\partial t}+u\frac{\partial v}{\partial x}+v\frac{\partial v}{\partial y}\right)=-\frac{\partial p}{\partial y}+\mu_{nf}\left(\frac{\partial^2 v}{\partial x^2}+\frac{\partial^2 v}{\partial y^2}\right) \tag{3}$$

$$\frac{\partial T}{\partial t}+u\frac{\partial T}{\partial x}+v\frac{\partial T}{\partial y}=\alpha_{nf}\left(\frac{\partial^2 T}{\partial x^2}+\frac{\partial^2 T}{\partial y^2}\right) \tag{4}$$

where, $\rho_{nf}=(1-\phi)\rho_f+\phi\rho_s$ is the density,

$(\rho C_p)_{nf}=(1-\phi)(\rho C_p)_f+\phi(\rho C_p)_s$ is the heat capacitance,

$\beta_{nf}=(1-\phi)\beta_f+\phi\beta_s$ is the thermal expansion coefficient,

$\alpha_{nf}=k_{nf}/(\rho C_p)_{nf}$ is the thermal diffusivity,

$\mu_{nf}=\mu_f(1-\phi)^{-2.5}$ is dynamic viscosity and

$k_{nf}=k_f\dfrac{k_s+2k_f-2\phi(k_f-k_s)}{k_s+2k_f+\phi(k_f-k_s)}$ is the thermal conductivity of the nanofluid.

The boundary conditions are:

at the upper and lower surfaces: $T=T_h$

at the inlet opening: $T=T_i$, $u=U_i$

at the remaining boundaries: $\dfrac{\partial T}{\partial n}=0$

at all solid boundaries: $u=v=0$

at the outlet opening convective boundary condition: $p=0$

The movement of the valve is described with an analytic expression *pin*, which returns the value of one in the area corresponding to the valve pin and zero elsewhere. The viscosity is then expressed by

$$\mu_{nf}=\mu_f(1-\phi)^{-2.5}+pin.\mu_\infty \tag{5}$$

where μ_f is the fluid viscosity, μ_∞ is a very large viscosity (ideally infinite), and pin is described by

$$pin=x_{pin}y_{pin} \tag{6}$$

where $x_{pin}=(x>x_0)(x<x_1)$

$y_{pin}=1-(y>y_1)+(y>y_2)$

y_1 and y_2 depend on time, *t,* according to:

$$y_1=-y_0+y_{\max}\,Sin(2\pi t) \tag{7}$$

$$y_1=y_0+y_{\max}\,Sin(2\pi t) \tag{8}$$

and where y_0, x_0, x_1, and $y_{\max}$ are fixed in time and describe the size of the valve pin and the amplitude with which the pin moves.

The above equations are non-dimensionalized by using the following dimensionless dependent and independent variables

$$X=\frac{x}{L},\quad Y=\frac{y}{L},\quad U=\frac{u}{U_i},\quad \tau=\frac{t}{U_i},\ V=\frac{v}{U_i},\quad P=\frac{p}{\rho_f U_i^{\,2}},\quad \theta=\frac{T-T_i}{T_h-T_i}$$

After substitution of the above variables into the equations (1) to (4), we get the following non-dimensional equations as

$$\frac{\partial U}{\partial X}+\frac{\partial V}{\partial Y}=0 \tag{9}$$

$$\frac{\partial U}{\partial \tau}+U\frac{\partial U}{\partial X}+V\frac{\partial U}{\partial Y} = -\frac{\rho_f}{\rho_{nf}}\frac{\partial P}{\partial X}+Pr\frac{\nu_{nf}}{\nu_f}\left(\frac{\partial^2 U}{\partial X^2}+\frac{\partial^2 U}{\partial Y^2}\right) \tag{10}$$

$$\frac{\partial V}{\partial \tau}+U\frac{\partial V}{\partial X}+V\frac{\partial V}{\partial Y} = -\frac{\rho_f}{\rho_{nf}}\frac{\partial P}{\partial Y}+Pr\frac{\nu_{nf}}{\nu_f}\left(\frac{\partial^2 V}{\partial X^2}+\frac{\partial^2 V}{\partial Y^2}\right) \tag{11}$$

$$\frac{\partial \theta}{\partial \tau}+U\frac{\partial \theta}{\partial X}+V\frac{\partial \theta}{\partial Y} = \frac{1}{Re\,Pr}\left(\frac{\partial^2 \theta}{\partial X^2}+\frac{\partial^2 \theta}{\partial Y^2}\right) \tag{12}$$

where $Pr=\frac{\nu_f}{\alpha_f}$ is Prandtl number and $Re=\frac{U_i L}{\nu_f}$ is Reynolds number.

The corresponding boundary conditions then take the following form:
at the upper-lower boundaries: $\theta=1$
at the inlet: $\theta=0$, $U=1$
at the outlet: convective boundary condition: $P=0$
at remaining boundaries: $\frac{\partial \theta}{\partial N}=0$
at all solid boundaries: $U=V=0$

The local Nusselt number at the heated surface of the valve may be expressed as

$$Nu_{local}=-\left(\frac{k_{nf}}{k_f}\right)\frac{\partial \theta}{\partial N} \tag{13}$$

The average Nusselt number takes the following form

$$Nu=\frac{1}{S}\int_0^S Nu_{local}\,dN \tag{14}$$

where $\frac{\partial \theta}{\partial N}=\frac{1}{L}\sqrt{\left(\frac{\partial \theta}{\partial X}\right)^2+\left(\frac{\partial \theta}{\partial Y}\right)^2}$ and S, N are the non-dimensional length and coordinate along the heated surface respectively.

The mean temperature of the fluid is $\theta_{av}=\int \theta\, d\overline{V}/\overline{V}$ (15)

where $\overline{V}$ is the volume of the fluid valve channel.

4. Numerical Technique

The Galerkin finite element method of Taylor and Hood (1973) and Dechaumphai (1999) is used to solve the non-dimensional governing equations along with boundary conditions for the considered problem. The equation of continuity has been used as a constraint due to mass conservation and this restriction may be used to find the pressure distribution. The penalty finite element method of Basak et al. (2009) is used to solve the Eqs. (2) - (4), where the pressure P is eliminated by a penalty constraint. The continuity equation is automatically fulfilled for large values of this penalty constraint. Then the velocity components (U, V), and temperature (θ) are expanded using a basis set. The Galerkin finite element technique yields the subsequent nonlinear residual equations. Three points Gaussian quadrature is used to evaluate the integrals in these equations. The non-linear residual equations are solved using Newton–Raphson method to determine the coefficients of the expansions. The convergence of solutions is assumed when the relative error for each variable between consecutive iterations is recorded below the convergence criterion ε such that $\left|\psi^{n+1}-\psi^{n}\right|\le 10^{-4}$, where n is the number of iteration and Ψ is a function of U, V, and θ.

4.1. Mesh Generation

In finite element method, the mesh generation is the technique to subdivide a domain into a set of sub-domains, called finite elements, control volume etc. The discrete locations are defined by the numerical grid, at which the variables are to be calculated. It is basically a discrete representation of the geometric domain on which the problem is to be solved. The computational domains with irregular geometries by a collection of finite elements make the method a valuable practical tool for the solution of boundary value problems arising in various fields of engineering. Fig. 2 displays the finite element mesh of the present physical domain.

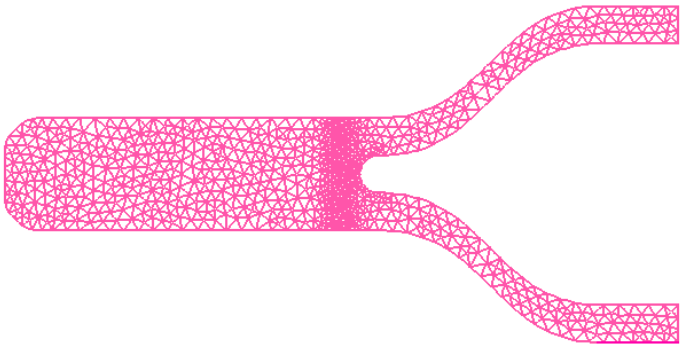

Fig. 2: Mesh generation of the fluid valve

4.2. Grid Refinement Test

In order to determine the proper grid size for this study, a grid independence test is conducted with five types of mesh for Pr = 1.47, Re = 100 and ϕ = 5%. The extreme value of Nu is used as a sensitivity measure of the accuracy of the solution and is selected as the monitoring variable. Considering both the accuracy of numerical value and computational time, the present calculations are performed with 12666 nodes and 8657 elements grid system. This is described in Fig. 3 and Table 1.

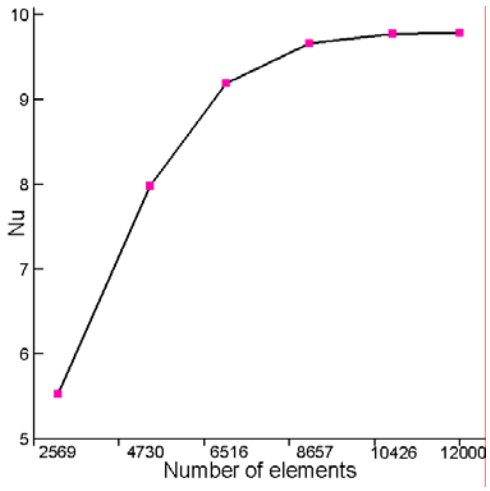

Fig. 3: Grid independency study for *Pr* = 1.47, *Re* = 100, and ϕ = 5%

Table 1: Grid Sensitivity Check at *Pr* = 1.47, *Re* = 100 and ϕ = 5%

Nodes (elements)	3224 (2569)	5982 (4730)	8538 (6516)	12666 (8657)	20524 (10426)	26008 (12000)
Nu	5.52945	7.98176	9.18701	9.6566249	9.7666249	9.779452
Time (s)	226.265	292.594	388.157	421.328	627.375	806.424

4.3. Thermophysical Properties

The thermo-physical properties of fluid (water) and solid CuO are tabulated in Table 2. The properties are taken from Yu et al. (2011).

Table 2: Thermo-physical properties of water-CuO nanofluid

Physical properties	water	CuO
C_p	4182	540
ρ	998.1	6510
k	0.6	18
β	2.2×10^{-4}	8.5×10^{-6}

5. Results and Discussion

In this section, numerical results in terms of streamlines and isotherms for transient analysis with the variation of Prandtl number are displayed, while Reynolds number *Re* and solid volume fraction ϕ are fixed at 100 and 5% respectively. In addition, the values of the local and average Nusselt number, average bulk temperature and subdomain velocity with time have been calculated for both water and water-CuO nanofluid.

5.1. Velocity Field

The Prandtl number effect on velocity field (modulus of the velocity vector) when the valve is completely open is displayed in Figs. 4-6. These figures present the flow development as a function of time is used for the cases of nanofluid and base fluid. Firstly, the Fig. 4 (*Pr* = 1.47) shows that the inlet is smaller than the compartment that it enters, so that some distance is required before the flow reaches another parabolic profile for the main body of the inlet chamber. In the velocity vector, some recirculation occurring at the corners of the chamber beside the inlet is visible. The structure of the outlet channels leads to a slight thinning toward the middle of the channels. This provides a slight acceleration and subsequently greater velocity magnitude in these regions.

Secondly, the occurring non-dimensional time of undershoot is chosen as the measure for the development time of the convective flow due to the increasing values of *Pr* from 1.47 to 3.77. Fig. 5 claims that the vortices created in the velocity field (for *Pr* = 1.47) disappear. The time instant for undershoot is decreased, while the trough value is increased with increasing time. At higher time the development of flow is nearly identical for both type of fluids. The deviation slightly grows as the time is decreased such that in case of nanofluid the flow always takes the longest time to develop.

Again increasing *Pr* upto 6.2, more perturbation is observed in the streamlines at time $\tau = 0.001$ and this tradition is maintained until steady state reached. Moreover, initially the flow is laminar that is inflow enters from the left and exits from the upper and lower phases of the fluid valve. Due to increasing time there creates two tiny vortices near the opening inlet. In addition, velocity field changes its pattern near the lower to upper position of the valve pin. Finally, at time $\tau \geq 0.1$ the flow becomes steady.

5.2. Temperature Field

Figs. 7-9 depict the thermal development as a function of time used for both water- CuO nanofluid and clear water. At the primary stage of time the thermal current activities are identical for both fluids at *Pr* = 1.47 (Fig. 7). The isotherms are clustered near the upper and lower hot surfaces. The deviation slightly grows as the time is increased such that in case of clear water the thermal field always takes the longest time to develop thermal boundary layer near the heated surfaces. Sequentially the isotherms dissipated from the heated boundaries and occupy the bulk of the fluid valve. The thermal plume develops at the inlet rapidly for nanofluid where as it takes time for nanofluid. After time $\tau = 0.1$ there is no variation in the isothermal lines so that steady state pattern is observed.

With the escalating values of *Pr* (= 3.77 and 6.2) as shown in Fig. 8 and 9, more heat is transferred by water-CuO nanofluid rather than the base fluid (ϕ = 0%). At initial stage ($\tau = 0.001$), the fluids carry heat from upper and lower heated surfaces of the fluid valve. In addition, the isothermal lines go the last edge of the both outlet exits for the time $\tau = 0.1$(steady state) whereas they can't at *Pr* = 1.47. Because, highly viscous fluid can transfer more heat.

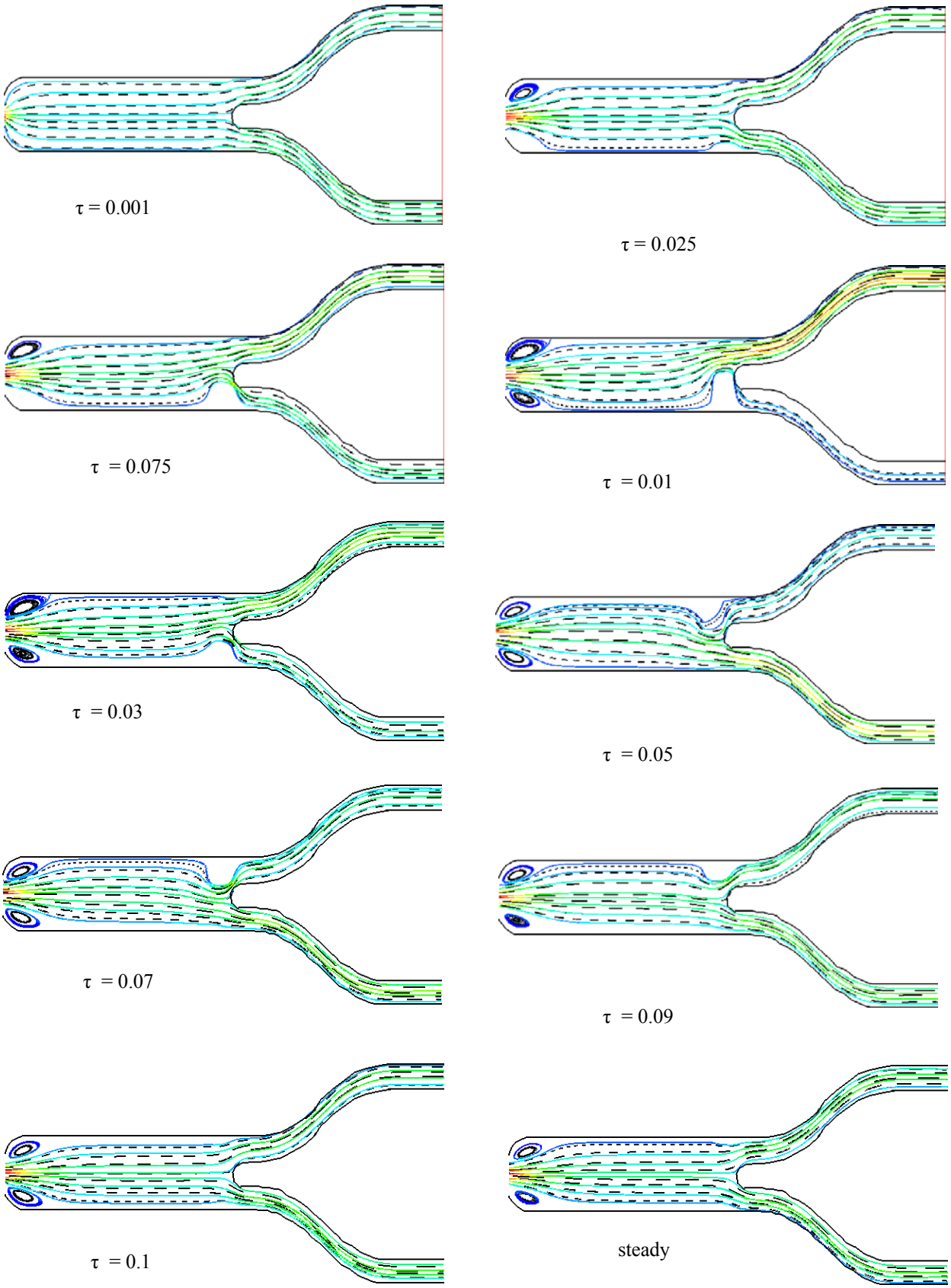

Fig. 4: Transient behavior of streamlines at *Pr* = 1.47 (nanofluid = solid lines and base fluid = dashed lines)

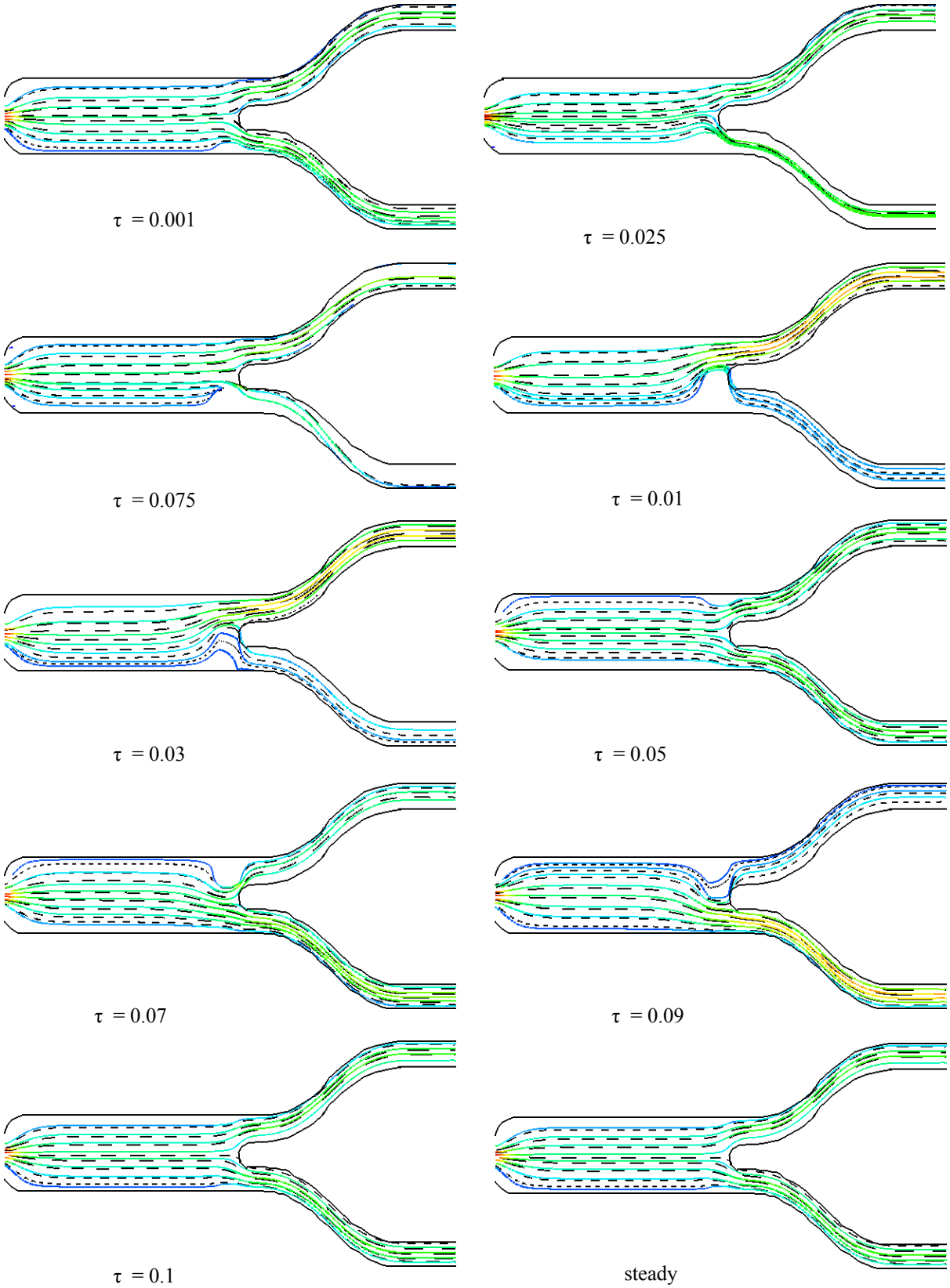

Fig. 5: Transient behavior of streamlines at *Pr* = 3.77 (solid lines for nanofluid and dashed lines for base fluid)

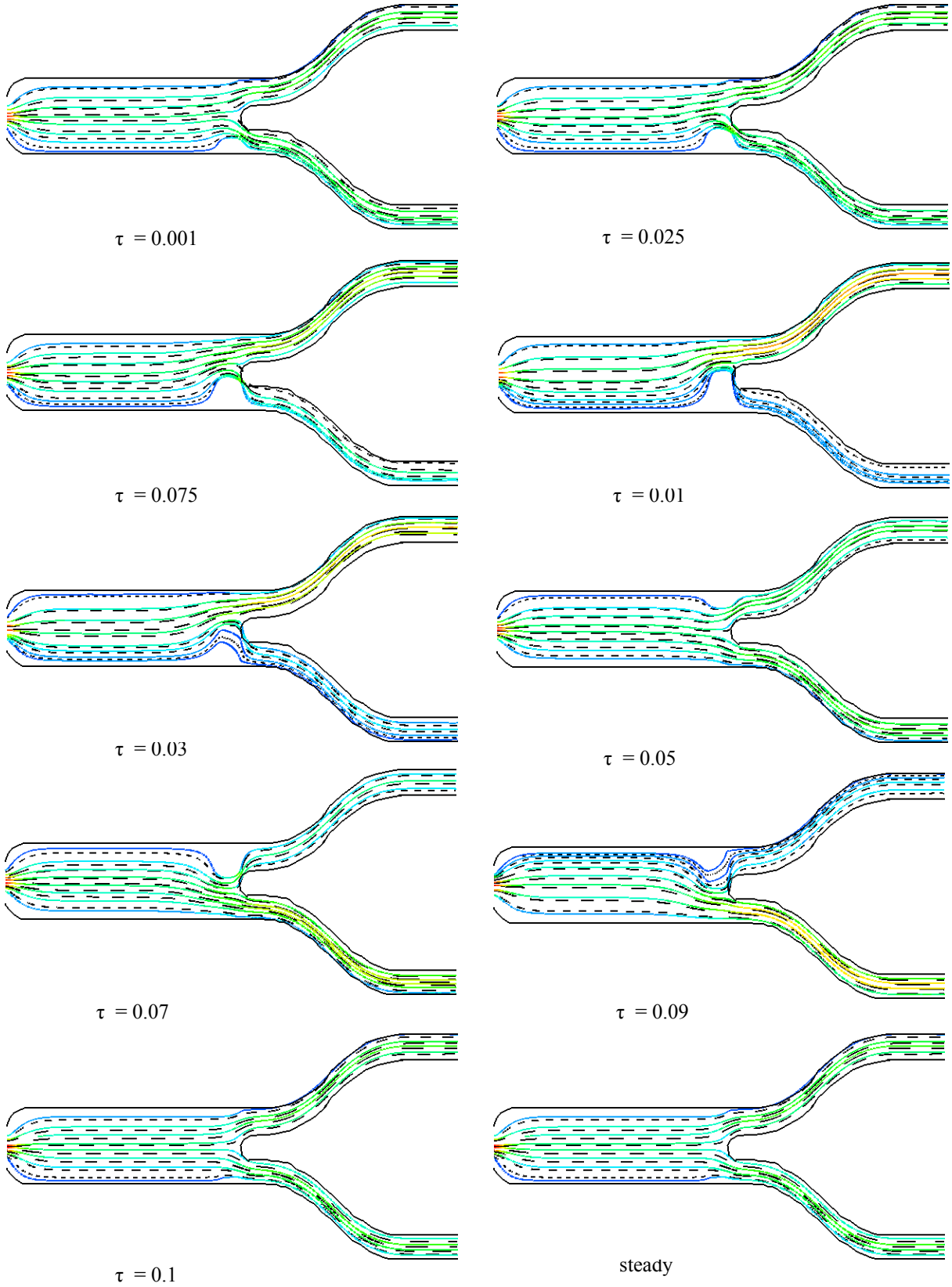

Fig. 6: Transient behavior of streamlines at *Pr* = 6.2 (solid lines for nanofluid and dashed lines for base fluid)

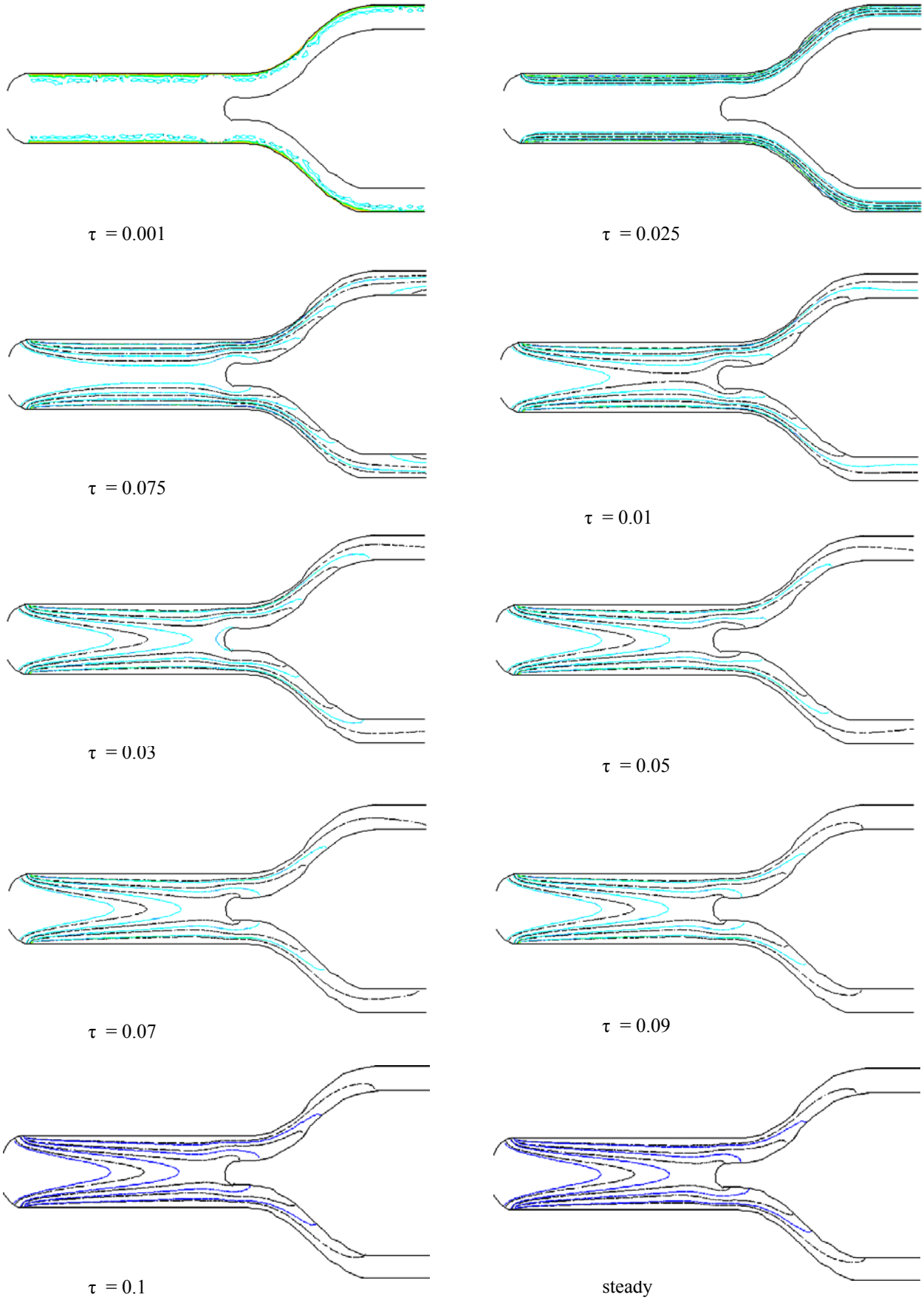

Fig. 7: Transient behavior of isotherms at *Pr* = 1.47 (solid lines for nanofluid and dashed lines for base fluid)

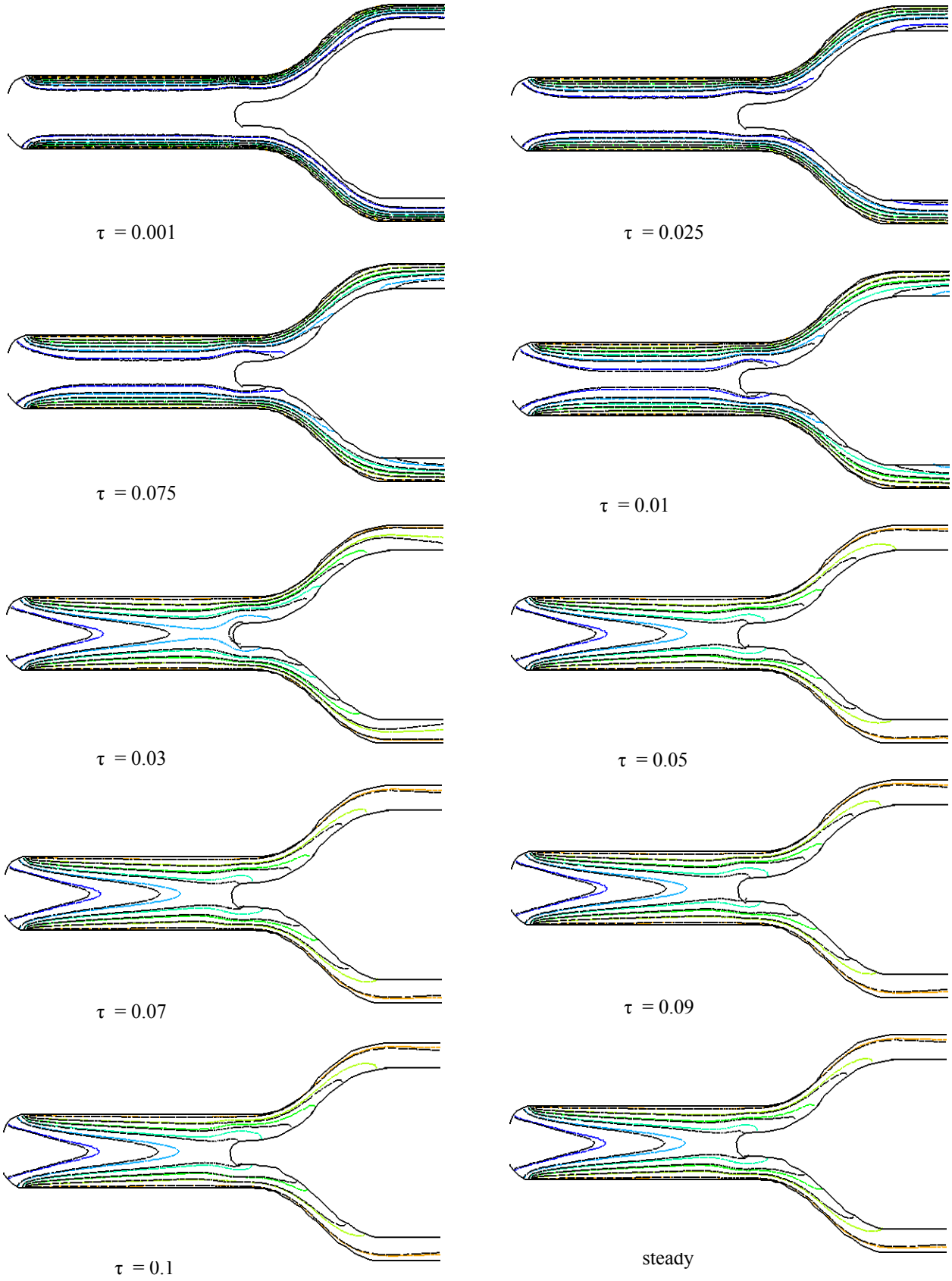

Fig. 8: Transient behavior of isotherms at *Pr* = 3.77 (solid lines for nanofluid and dashed lines for base fluid)

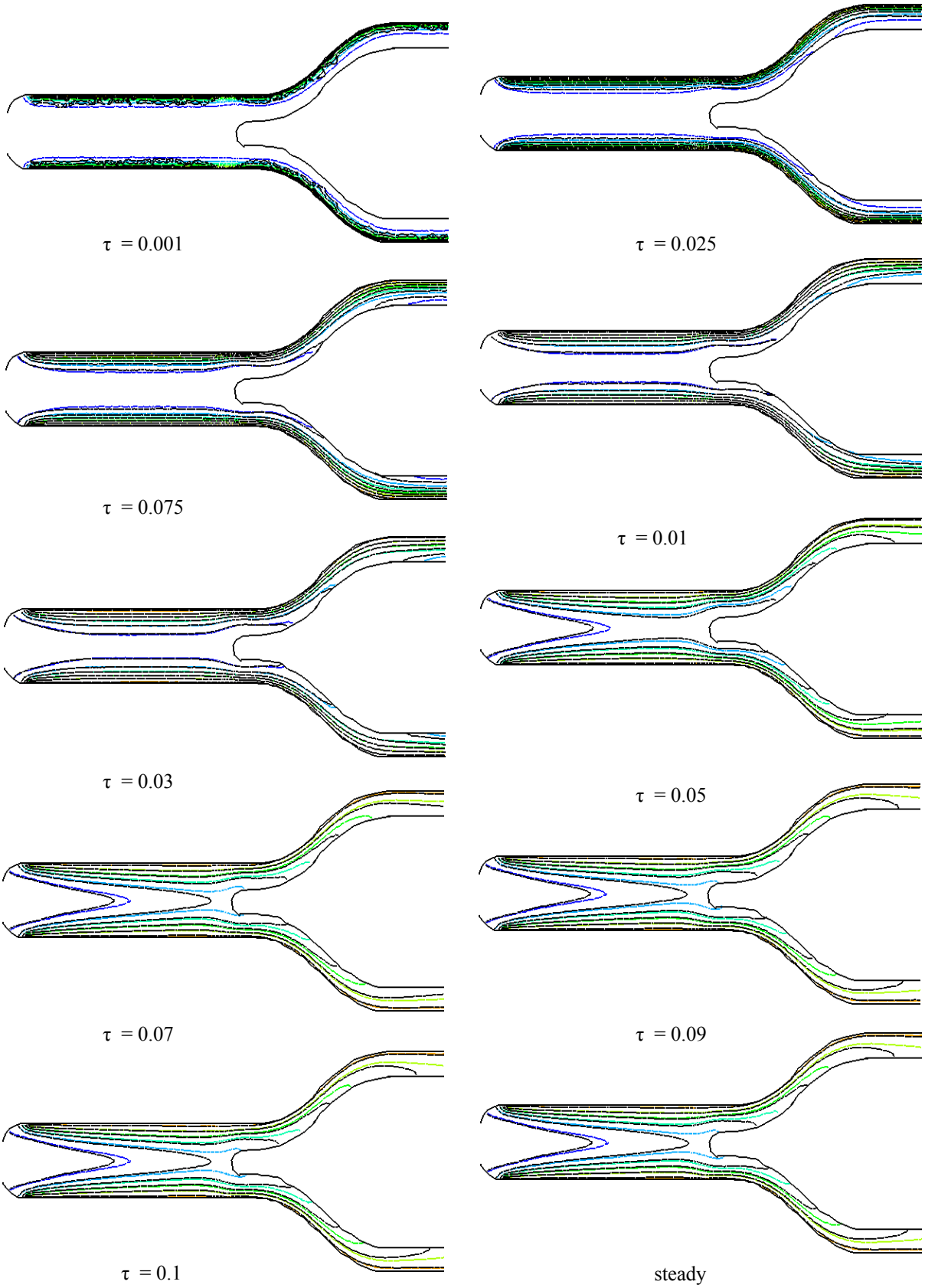

Fig. 9: Transient behavior of isotherms at *Pr* = 6.2 (solid lines for nanofluid and dashed lines for base fluid)

5.3. Heat Transfer Coefficients

In the present study, the local Nusselt number (Nu_{local}) along with X-axis for both upper and lower phases of the fluid valve is offered in Fig. 10(i)-(ii). With increasing X, the local Nusselt number decreases due to decrement of temperature difference and increment of thickness of boundary layer for both type of fluids. Local Nusselt number becomes relative maximum at the peaks which results in increment of compression of isotherms. The Prandtl number- Nu_{local} profile rises due to escalating values of *Pr* from 1.47 to 6.2. In all cases, Nu_{local} is seen to be higher for water-CuO nanofluid than base fluid.

The time-averaged Nusselt number is obtained by computing the time average of the average Nusselt number over the hot surfaces for a process, given by total time being the duration of the process of interest. *Nu* is obtained at the lower phase of the fluid valve. Fig. 11(i) expresses that the average Nusselt number decreases with higher time and lower Prandtl number for both cases whereas the nanofluid has greater heat transfer rate than the base fluid. This is because, the fluid with the highest Prandtl number is capable to carry more heat away from the heated surfaces and dissipated through the out flow opening.

It is observed from Fig. 11 (ii) that the average fluid temperature increases for rising values of time upto $\tau \leq 0.03$. Then it is almost identical with the variation of time. Initially bulk temperature of both fluids is same but variation observed within them with rising dimensionless time. θ_{av} devalues with respect to the growing *Pr*. Higher temperature is found for nanofluid at *Pr* = 1.47.

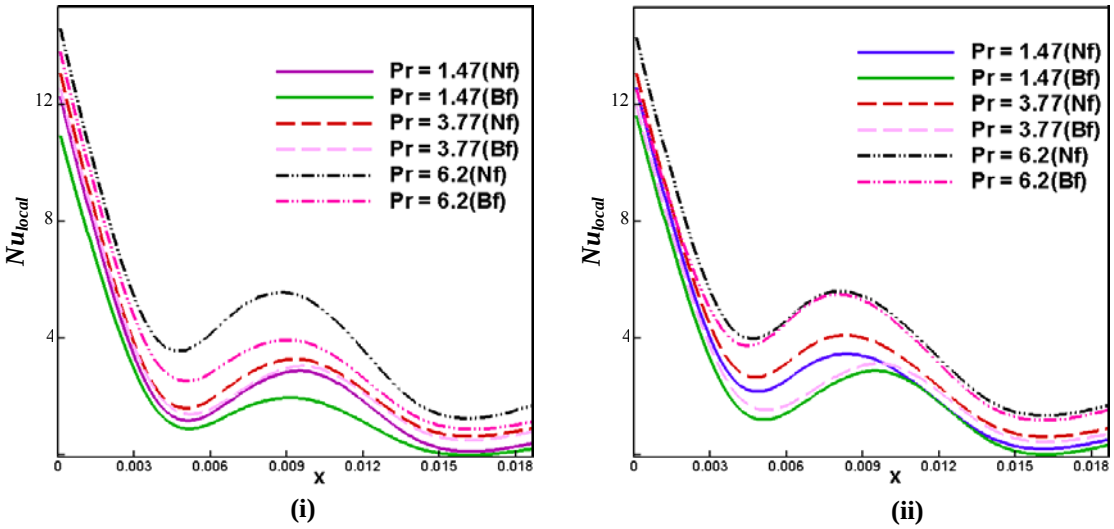

Fig. 10: Effect of *Pr* on local Nusselt number at (i) upper phase and (ii) lower phase (Nf = nanofluid, Bf = base fluid)

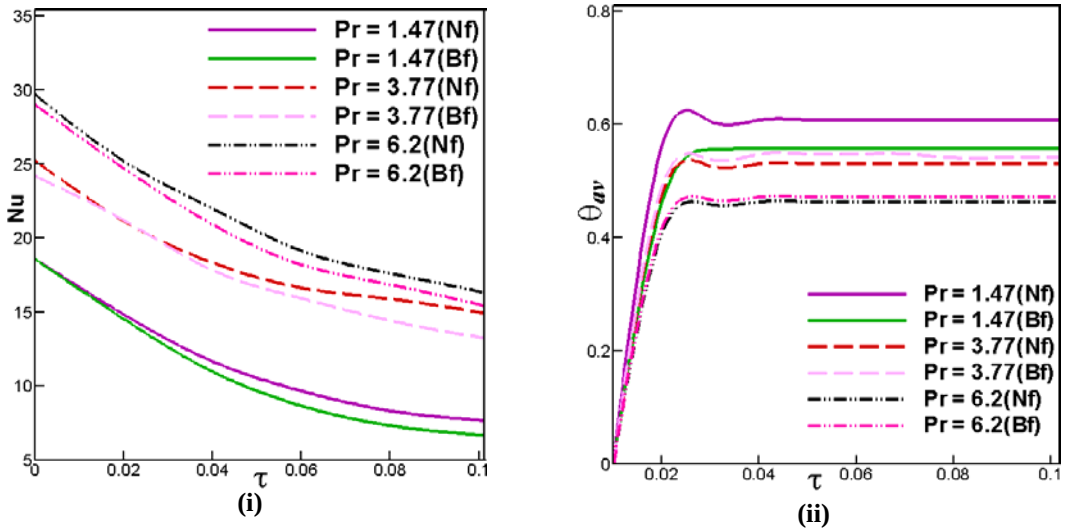

Fig. 11: Effect of *Pr* on (i) *Nu* and (ii) θ_{av} (Nf = nanofluid, Bf = base fluid)

5.4. Velocity Field

Fig. 12 shows a plot of the subdomain velocity as a function of time in the fluid valve. For both nanofluid and pure water, the figure illustrates the periodic flow due to the periodic motion of the valve pin. The results predicted by neglecting the Brownian motion effects are compared with those obtained by taking the Brownian motion effects into consideration. It is seen that the wave amplitude for clear water is found greater with compared to the water-CuO nanofluid. This happens due to the fact that the base fluid moves more rapidly than the nanofluid. The velocity field diminishes sequentially with mounting *Pr* due to high viscosity of the fluid.

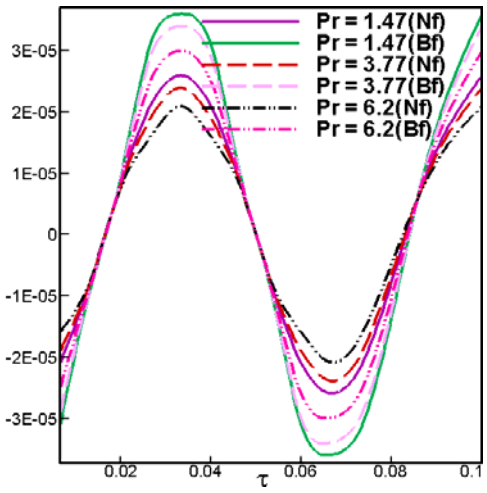

Fig. 12: Plot of subdomain velocity for various *Pr*
(Nf = nanofluid, Bf = base fluid)

6. Conclusion

The problem of Prandtl number effect on the transient forced convection heat transfer in a valve filled with water-CuO nanofluid has been studied numerically. Flow and temperature field in terms of streamlines and isotherms have been considered for various Prandtl number and dimensionless time until the steady state observed. The results of the numerical analysis lead to the following conclusions:

- The structure of the fluid flow and temperature field within the fluid valve is found to be significantly dependent upon the time (τ).
- Vortices created by low viscosity in the streamlines disappear and thermal layer near the heated surface become thick with increasing values of *Pr*.
- The CuO nanoparticles is established to be most effective in enhancing performance of heat transfer rate at the highest *Pr*.
- The mean temperature of the fluid in the fluid valve increases with dimensionless time as well as for the lowest *Pr*. In comparison water-CuO nanofluid achieves the higher temperature than the base fluid.

Nomenclature

C_p	Specific heat at constant pressure ($KJkg^{-1}K^{-1}$)
k	Thermal conductivity ($Wm^{-1}K^{-1}$)
L	Length of the fluid valve (m)
Nu	Nusselt number
p	Dimensional pressure (Nm^{-2})
P	Non-dimensional pressure
Pr	Prandtl number
Re	Reynolds number
T	Dimensional temperature (K)

u, v	Velocity components (ms^{-1}) along x, y direction respectively
U, V	Dimensionless velocity components along X, Y direction respectively
x, y	Cartesian coordinates (m)
X, Y	Non-dimensional Cartesian coordinates
Greek symbols	
α	Thermal diffusivity (m^2s^{-1})
β	Thermal expansion coefficient (K^{-1})
ϕ	Solid volume fraction
θ	Non-dimensional temperature
μ	Dynamic viscosity of the fluid (Kg $m^{-1}s^{-1}$)
ν	Kinematic viscosity of the fluid (m^2s^{-1})
ρ	Density of the fluid (Kg m^{-3})
Subscripts	
f	Base fluid
h	Heated wall
i	Inlet state
nf	Water-CuO nanofluid
s	Solid particle

References

Abu-Nada, E., Masoud, Z., Oztop, H.F., Campo, A., 2010. Effect of nanofluid variable properties on natural convection in enclosures, *International Journal of Thermal Sciences*, Vol. 49, pp. 479–491.

Abu-Nada, E., Oztop, H.F., 2009. Effects of inclination angle on natural convection in enclosures filled with Cu–water nanofluid, *International Journal for Heat & Fluid Flow*, Vol. 30, pp. 669–678.

Basak, T., Roy, S., Pop, I., 2009. Heat flow analysis for natural convection within trapezoidal enclosures based on heatline concept, *Int. J. Heat Mass Transfer*, Vol. 52, pp. 2471–2483.

Chen, X., Li, J. M., Dai, W. T. and Wang, B. X., 2004. Enhancing convection heat transfer in mini tubes with nanoparticle suspensions, *J. Eng. Thermophys.*, Vol. 25, No. 4, pp. 643–645.

Dai, W. T., Li, J. M., Chen, X. and Wang, B. X., 2003. Experimental investigation on convective heat transfer of copper oxide nonoparticle suspensions inside mini-diameter tubes, *J. Eng. Thermophys.*, Vol. 24, No. 4, pp. 633–636.

Dai, W. T., Li, J. M., Wang, B. X. and Chen, X., 2002. An experimental study on the flow and heat transfer characteristics of copper oxide nanoparticle suspensions inside mini-diameter tube, *Ind. Heating,*, Vol. 5, pp. 1–4.

Das, M.K., Ohal, P.S., 2009. Natural convection heat transfer augmentation in a partially heated and partially cooled square cavity utilizing nanofluids, *International Journal of Numerical Methods for Heat & Fluid Flow*, Vol. 19, No. 1, pp. 411–431.

Dechaumphai, P., Finite Element Method in Engineering, 2nd ed., Chulalongkorn University Press, Bangkok, 1999.

Ghasemi, B., Aminossadati, S.M., 2009. Natural convection heat transfer in an inclined enclosure filled with a water–CuO nanofluid, *Numerical Heat Transfer Part A*, Vol. 55, pp. 807–823.

Kumar, S., Prasad, S.K., Banerjee, J., 2009. Analysis of flow and thermal field in nanofluid using a single phase thermal dispersion model, *Applied Mathematical Modelling*, Vol. 34, pp. 573–592.

Lin, K. C., Violi, A., 2010. Natural convection heat transfer of nanofluids in a vertical cavity: Effects of non-uniform particle diameter and temperature on thermal conductivity, *International Journal of Heat and Fluid Flow*, Vol. 31,pp. 236–245

Liu, Z. H. and Liao, L., 2008. Sorption and agglutination phenomenon of nanofluids on a plain heating surface during pool boiling, *Int. J. Heat Mass Transfer*, Vol. 51, No. 9–10, pp. 2593–2602.

Muthtamilselvan, M., Kandaswamy, P., Lee, J., 2009. Heat transfer enhancement of copper–water nanofluids in a lid-driven enclosure, *Communications in Nonlinear Science and Numerical Simulation*, Vol. 15, No. 6, pp. 1501–1510.

Ogut, E.B., 2009. Natural convection of water-based nanofluids in an inclined enclosure with a heat source, *International Journal of Thermal Sciences*, Vol. 48, pp. 2063–2073.

Pfautsch, E., Forced convection in nanofluids over a flat plate, Thesis Presented to the Faculty of the Graduate School, University of Missouri, 2008.

Putra, N., Roetzel, W., Das, S.K., 2003. Natural convection of nano-fluids, *Heat and Mass Transfer*, Vol. 39, pp. 775–784.

Saleh, H., Roslan, R., Hashim, I., 2011.Natural convection heat transfer in a nanofluid-filled trapezoidal enclosure, *International Journal of Heat and Mass Transfer*, Vol. 54, pp. 194–201.

Santra, A.K. , Sen, S., Chakraborty, N., 2008. Study of heat transfer augmentation in a differentially heated square cavity using copper–water nanofluid, *International Journal of Thermal Sciences*, Vol. 47, pp. 1113–1122.

Santra, A.K., Sen, S., Chakraborty, N., 2008. Study of heat transfer characteristics of copper–water nanofluid in a differentially heated square cavity with different viscosity models, *Journal of Enhanced Heat Transfer*, Vol. 15, No. 4, pp. 273–287.

Taylor, C., Hood, P., 1973. A numerical solution of the Navier-Stokes equations using finite element technique, *Computer and Fluids*, Vol. 1, pp. 73–89.

Wen D. S. and Ding, Y. L, 2004. Experimental investigation into convective heat transfer of nanofluids at entrance area under laminar flow region, *Int. J. Heat Mass Transfer*, Vol. 47, pp. 5181–5188.

Wong, K.F.V., Bon, B.L., Vu, S., Samedi, S., 2008. Study of nanofluid natural convection phenomena in rectangular enclosures, *ASME Int. Mech. Eng. Cong. Exposition, Proc.* 6, pp. 3–13.

Yu, Zi-Tao, Xu Xu, Hu, Ya-Cai, Fan, Li-Wu, Cen, Ke-Fa, 2011. Numerical study of transient buoyancy-driven convective heat transfer of water-based nanofluids in a bottom-heated isosceles triangular enclosure, *International Journal of Heat and Mass Transfer*, Vol. 54, pp. 526–532.

Biographical notes

Rehena Nasrin received M. Sc. and M. Phil. from University of Dhaka and Bangladesh University of Engineering and Technology, Bangladesh in 2002 and 2009, respectively. Now she is Assistant Professor in the Department of Mathematics, Bangladesh University of Engineering and Technology, Bangladesh. Now she is a Ph. D. student in Nanofluid with Computational Fluid Dynamics.

M. A. Alim received M. Phil. and Ph. D. from Bangladesh University of Engineering and Technology, Bangladesh and Loughborough University, Loughborough, Leicestershire, UK respectively. Now he is Associate Professor in the Department of Mathematics, Bangladesh University of Engineering and Technology, Bangladesh. He is reviewer of more than twenty five international journals.

Ali J. Chamkha is Professor of Manufacturing Engineering Department, The Public Authority for Applied Education and Training, Shuweikh 70654, Kuwait. His current area of research includes Computational Fluid Dynamics, Quality Engineering, Nanofluids and Nanoparticles, Numerical Heat and Mass Transfer and Simulation. He has published more than seventy papers in referred international journals. He has also presented more than one hundred research articles in national and international conferences.

Received January 2012
Accepted February 2012
Final acceptance in revised form March 2012